Dalton Transactions

Accepted Manuscript

ROYAL SOCIETY OF CHEMISTRY

www.rsc.org/dalton

Artificial hemes for DSSC and/or BHJ applications

Kalliopi Ladomenou, Vasilis Nikolaou, Georgios Charalambidis, Athanassios G. Coutsolelos*

Chemistry Department

University of Crete

Voutes Campus, PO Box 2208, 70013 Heraklion, Crete, Greece.

E-mail: acoutsol@uoc.gr

Contents

Abbreviations:

BHJ = bulk Heterojuction

bipy = 2,2'-bipyridine

BODIPY = 4,4-difluoro-4-bora-3a,4a-diaza-s-indacene

CB = conduction band

CDCA = chenodeoxycholic acid

CT =charge transfer

DCA = deoxycholic acid

DFT = density functional theory

DSSCs = dye sensitized solar cells

EIS = electrochemical impedance spectroscopy

EPD = electrophoretic deposition

FF = fill factor

FTO = fluorine-doped tin oxide

ICT = intramolecular charge transfer

IPCE = incident Photon to Current Efficiency

J_{sc} = short circuit current

LHE = light harvesting efficiency

LUMO = lowest unoccupied molecular orbital

PC = paste-coating

PCE = power conversion efficiency

rGO = reduced graphene oxide

V_{oc} = open circuit voltage

τ_e = electron lifetime

Abstract

In recent years solar to power energy conversion devices have been attracted a lot of attention and there is an effort to synthesize novel light-harvesting organic materials. Inspired by nature and due to their remarkable role in photosynthesis, porphyrins have been extensively used for DSSC and BHJ applications. This review provides a summary of the developments and approaches that were used in our group in order to improve the power conversion efficiency of DSSCs and BHJs based on porphyrin hybrid derivatives. Aiming to extend the light absorption range of the sensitizing dyes and to achieve enhanced solar cell performances, functionalized porphyrins with carboxylic acid anchoring groups were synthesized. These include monomeric, dimeric and trimeric porphyrins with one or two anchoring groups and with the presence of an additional chromophore in some examples. Also, porphyrins with pyridyl anchoring groups were studied, in order to examine the influence in the power conversion efficiency of a different anchoring group. The photovoltaic properties were improved after reduction of dye-aggregation by means of chemical co-adsorbents, and by using co-sensitization, modified photoanodes and electrolyte additives. Finally, some of the above chromophores were used as electron donors for the preparation of a solution processed BHJ organic solar cell with the presence of various electron acceptors.

1. Introduction

In recent years there is an urgent need to use alternative energy supplies due to the increasing demand of energy and the depletion of fossil fuels. Among the renewable energy sources photovoltaic technology is an excellent alternative due to the abundance and the global character of the solar energy. Solar cells or photovoltaic cells, convert sunlight (photons) directly into electricity (voltage). At present most of the solar cells are fabricated from silicon, producing on average 20% of electricity.[1, 2] This type of solar cells has certain limitations concerning their high production cost and their large scale fabrication. For that reason, in order to improve the photovoltaic technology a new generation of more efficient, stable, low cost light harvesters must be prepared from readily available resources and lower environmental impact. New technologies such as Organic Photovoltaics and Dye Sensitized Solar Cells (DSSCs) could be an alternative to silicon based solar cells. They both appear advantages such as facile and low cost production, low weight and device flexibility. Despite these advances none of the two technologies can be used as alternative to fossil fuel consumption due to their low efficiencies around 13% for DSSC[3] and 10% for small molecules and polymer-fullerene Bulk Heterojuction (BHJ) solar cells.[4, 5] Therefore, further research is needed in order to increase the efficiencies of these two technologies.

In DSSC technology the light is absorbed by dye molecules, deposited on nanostructures such as titanium dioxide, zinc oxide or tin oxide. These nanoparticles are placed on an Indium Tin Oxide coated glass surface (anode). There is also a platinum cathode that sandwich together with a redox electrolyte (Fig. 1).[6]

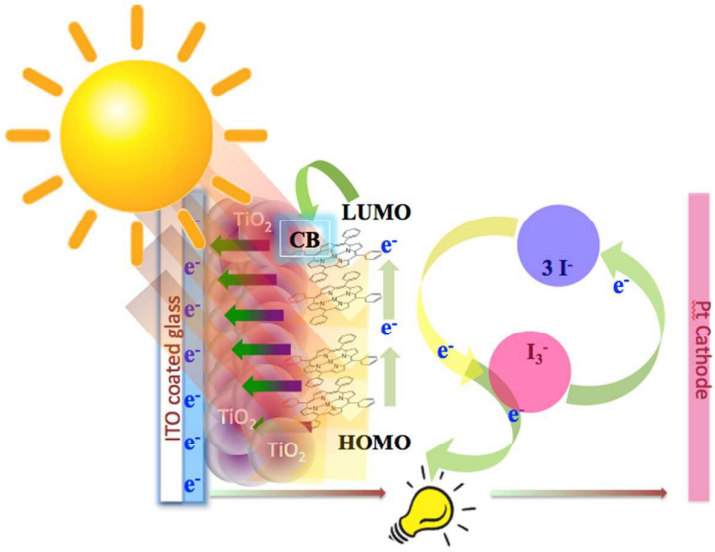

Fig. 1 Schematic representation of a DSSC.

Solar irradiation excites the electrons of the dye from HOMO to LUMO level. Then the electrons from LUMO orbitals are injected into the conduction band (CB) of the TiO_2 semiconductor and subsequently carried out to counter Pt-electrode through the external circuit and thus produce electricity. Dye regeneration is performed by an electrolyte (iodine-based or cobalt complexes, redox mediator) through a reduction–oxidation process. Dyes with donor–acceptor (D–A) groups having their LUMO level above the TiO_2 conduction band and their HOMO level below the redox couple of the electrolyte are desirable for electrochemical cycle in DSSC. Strong electronic coupling and physical contact is needed between the light harvesting chromophore and the semiconductor surface for faster excited state electron transfer than excitation quenching by other physicochemical processes, which reduces the efficiency of the cell.

The performance of a solar cell strongly depends on the light harvesting ability and the relative energy levels of the dye, as well as the kinetics of the charge transfer processes at different interfaces. In addition, the photo excitation of a D-A dye is followed by intramolecular charge transfer (ICT) from the donor to the acceptor moiety of the dye. The ICT property of a D-A dye is strongly dependent on the electron-donating ability of D, the electron-withdrawing ability of A, as well as the electronic properties of the π-conjugated bridge, and it can be

tuned through chemical modification of each component. Due to the D–A interaction, a new low energy molecular orbital (MO) is being formed. Facile excitation of the electrons within the new MO can be achieved using visible light and these type of molecules are usually referred as charge-transfer chromophores.[7-10] During the last decade, different arylamines, such as triphenylamine (TPA),[11, 12] coumarin[13, 14] indoline,[15, 16] and carbazole[17, 18] have been investigated as the electron-donating group. Most of them exhibited satisfactory electron-donating ability. Chromophores with the TPA moiety as the electron-donor have shown long-lived charge-separated state and good hole-transporting ability.[19, 20] In addition, its non-planar configuration with steric hindrance can be used to prevent the unfavorable aggregation on the TiO_2 surface. In the past few years, the dyes with TPA moiety have been widely investigated as sensitizers in DSSCs.[21-25] The conjugated linker in a D–π–A system acts as both a component for light harvesting and a channel for charge transport. A good conjugated linker should promote the absorption of light over a wide region, and at the same time, facilitate charge transfer.

Besides the electron-donor and π-conjugated linker, a push-pull system is completed by introducing an electron-acceptor. There are a number of different electron-acceptors reported so far and their electron-withdrawing abilities have a big influence on the optical properties and energy levels of the compounds.[26-28]

On the other hand bulk heterojunction organic solar cells (BHJ) have been extensively used since their introduction in 1995. A typical BHJ solar cell has a structure as shown in Fig. 2. The active layer is sandwiched between two electrodes, one transparent and one reflecting. The glass substrate is coated with indium-tin-oxide (ITO) which is a transparent conductive electrode with a high work function, suitable to act as an anode. To reduce the roughness of this ITO layer and increase the work function even further, a layer of poly(3,4-ethylene dioxythio-phene):poly(styrene sulfonate) (PEDOT:PSS) is spin cast, followed by the active layer. The top electrode usually consists of a low work function metal or lithium fluoride (LiF), topped with a layer of aluminum, all of which are deposited by thermal deposition in vacuum through a shadow mask. Moreover, the solution processed active layer consists of an electron donating and an

electron accepting material at a typical length scale of a few tens of nanometers.[29-31] Light absorption results in the formation of singlet excitons that diffuse to the donor-acceptor interface to form interfacial charge transfer (CT) excited state species that can dissociate into free holes and electrons (as electrons fall from the donor conduction band to the acceptor conduction band), which are finally directed to the corresponding electrodes, generating current (Fig. 2).

In this review paper we present the research from our group on the use of porphyrins as light harvesters in DSSCs and BHJ photovoltaic cells. Concerning the DSSCs studies two different anchoring groups were studied carboxylic acid and pyridine, attached onto different porphyrins. On the other hand, BHJ studies were done using some of the dyes that were already used in DSSCs measurements.

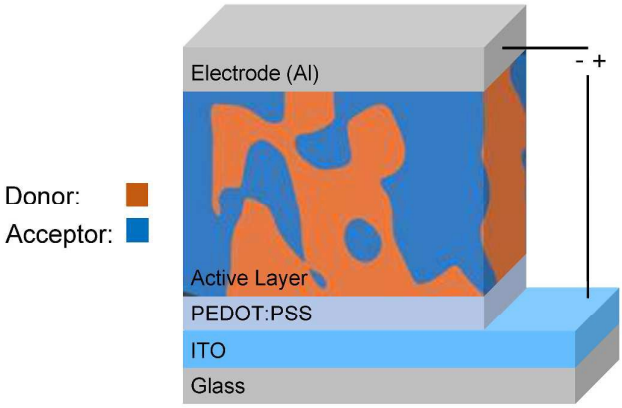

Fig. 2 Schematic representation of BHJ photovoltaic cells.

2. Porphyrins for DSSCs

Among various parameters of the DSSC device in achieving high efficiency and durability, the sensitizer is one of the key components. The leading dyes until recently in DSSC technology that showed the best efficiencies (up to 11%) were the ruthenium polypyridyl compounds.[32, 33] However, the high cost, toxicity and low stability of the ruthenium complexes led researchers to search for alternate chromophores such as, porphyrins, phthalocyanines and other organic dyes.

Inspired by nature and due to their remarkable role in photosynthesis, porphyrins have been extensively designed and synthesized for DSSC applications. Porphyrins as photosensitizers on DSSC are particularly interesting possessing various advantages such as appropriate LUMO and HOMO energy levels and very strong absorption of the Soret band in the 400–450 nm region, as well as the Q-bands in the 500–700 nm region. Moreover, the photophysical and electrochemical properties of the porphyrins can be tuned by inner metal complexations and peripheral substituents, by taking advantage of their multiple reactive sites, including four *meso* and eight β-positions (Chart 1).[34-40]

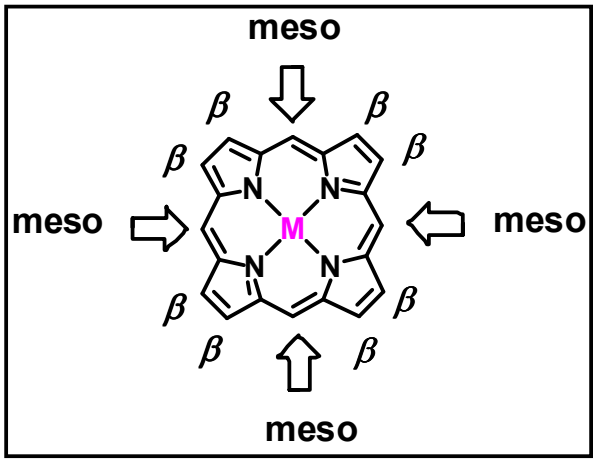

Chart 1 Schematic representation of *meso* and β positions of the porphyrin macrocycle.

A number of review articles on porphyrins, and their applications in photovoltaics have been reported covering most of the common features of the DSSC systems.[33, 41-48] Porphyrin derivatives that contain one donor moiety and one acceptor in *trans* position on the macrocycle are found to have the highest efficiencies recorded so far. The best efficiency ~13 % is achieved by the group of Grätzel in 2014 using donor-acceptor porphyrin with long alkyl chains in order to prevent aggregation.[3, 49] A drawback of porphyrins is the poor light-harvesting properties at wavelengths around 450 nm and above 600 nm. Elongation of strong electron-donating and electron-withdrawing groups can shift and broad the absorption of porphyrins making it possible to increase the light-harvesting property and the resulting DSSC efficiency. Therefore, the DSSC device

performance can be further improved by careful structural optimization of the porphyrin chromophores in order to exhibit a panchromatic feature.

Another approach to overcome the downside of low efficiency is co-sensitization. Therefore, the presence of an additional chromophore with complementary absorption properties could achieve highly efficient light harvesting and improved DSSC efficiency. On the other hand, when two different dyes are present may cause a decrease in efficiency. This may be due to the decreased injection efficiency caused by intermolecular interaction between the two chomophores. Furthermore, the co-sensitizer ideally may be able to reduce the porphyrin aggregates that are formed upon their attachment to TiO_2.

Furthermore, in DSSCs the presence of an anchoring group is essential to graft the dye on a TiO_2 surface, in order to achieve fast electron injection into the TiO_2 semiconductor.[50] The efficiency of the electron-transfer step at the dye-semiconductor interface is highly dependent, among numerous other factors, on the way the chromophore is attached to the surface.[51-53] Therefore, different porphyrin anchoring groups have been used and researchers have studied their effect on the TiO_2 surface.[54-56] In this report we will present carboxylic acid and pyridine anchoring groups that are prepared in our group.

2.1 Porphyrins for DSSC with carboxylic acid anchoring groups

Carboxylic acid present in the *meso* or *β*–positions of a porphyrin ring is an anchoring group that has been extensively studied. At the *meso*-position, two main classes of linking moieties have been employed most often, the classic *meso*-substituted benzoic acid linking and the direct attachment of a *meso*-alkynylbenzoic acid moiety. For DSSCs employing a *β*–position linking group the conjugated ones have been mostly reported in the literature. Carboxylic acid groups can form ester linkages with the surface of the metal oxide to provide a strongly bound dye and good electronic communication between the two parts. In this section porphyrin based chromophores bearing various carboxylic acids as anchoring groups will be presented.

2.1.1 Monomeric chromophores

In this first part we present monomeric porphyrin derivatives with carboxylic acids at the peripheries as anchoring groups to TiO_2. We synthesized a zinc-metallated porphyrin **1** with two carboxylate groups at the *meso* positions and two phenylene vinylene units at the other two *meso* positions, terminated by 4-nitro-α-cyanostilbene groups (Fig. 3).[57] The phenylene vinylene units expand the *π*-conjugation of **1**, leading to enhanced solubility and broadening of the absorption spectrum. The photophysical measurements revealed that the expanded conjugation of **1** resulted in broadening and strengthening of the Soret and Q bands of the porphyrin ring, improving the photovoltaic performance. The central porphyrin core acts as an electron donating unit and intramolecular charge transfer takes place to the electron withdrawing groups (4-nitro-α-cyanostibene). The power conversion efficiency (PCE) of **1** was measured 2.90% and with the addition of deoxycholic acid (DCA) was further improved to 4.22%. The presence of DCA decreased the dye loading and significantly increased the short circuit current (J_{sc}) and the open circuit voltage (V_{oc}). Those enhanced J_{sc} and V_{oc} values, are correlated with the increased electron injection efficiency and electron lifetime, respectively.

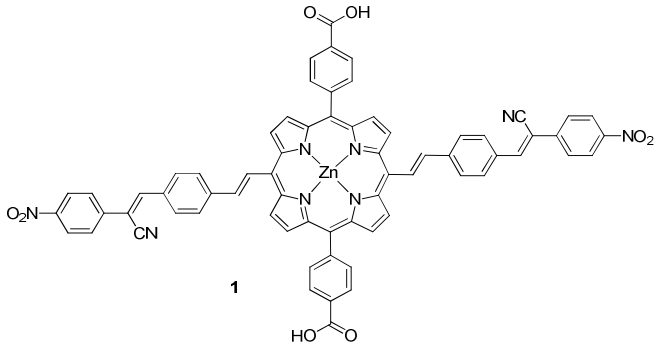

1

Fig. 3 Chemical structure of porphyrin **1**.

Following our previous strategy, we prepared two A_2B_2 type porphyrin compounds as sensitizers for DSSCs.[58] The free base porphyrin **2** and the corresponding zinc metallated complex **3** contain two carboxylate units and two N,N'-dimethylphenyl groups in *trans* position to the porphyrin macrocycle (Fig. 4). The latter can serve as electron donating group, while carboxylate units serve as electron accepting and as anchoring groups, verified from the Density Functional

Theory (DFT) calculations. Compounds **2** and **3** exhibit PCE values of 3.80% and 4.90% respectively. The increased PCE value of porphyrin **3** is due to higher dye loading onto TiO_2 and longer electron lifetime compared to **2**. When chenodeoxycholic acid (CDCA) was incorporated in the dye solution as co-adsorbent, the molecular aggregation on the TiO_2 surface was reduced and the PCE performances of both **2** and **3** were further improved to 4.90% and 6.07% respectively.[59] We also investigated the interfacial charge transfer of the DSSCs based on **2** and **3** with the addition of CDCA by electrochemical impedance spectroscopy (EIS). From the Nyquist plots we concluded that the electron transfer was improved in both cases upon co-adsorption with CDCA.

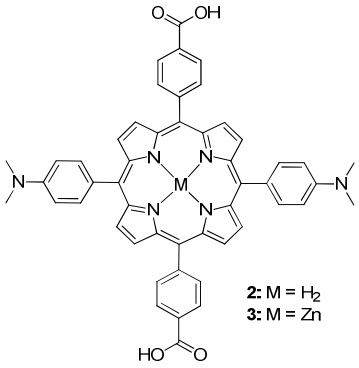

Fig. 4 Porphyrin derivatives **2** and **3**.

In the previous examples the two anchoring groups could not be both attached onto TiO2. Therefore, in order to study the influence of the attachment of two anchoring groups we synthesized a zinc porphyrin derivative consisting of two carboxylate units.[60] Porphyrin **4** is covalently linked through its peripheral aryl-amino group with a 1,3,5-triazine moiety, which contains two glycine units (Fig. 5). The glycine moieties at 3- and 5-positions possess carboxylic acids that act as anchoring groups for successful attachment on the TiO_2 surface. The PCE value of dye **4** was measured 4.72%, which is similar to the PCE value of porphyrin **3**. This result indicates that in this kind of compounds the position of the anchoring groups does not influence significantly the PCE values. The photovoltaic performance of **4** was enhanced by the addition of tertiary aryl

amine compound **5** (Fig. 5) functionalized with two ethynyl-pyridine substituents and one cyano-acetic acid group. Co-sensitization of **4** with **5** resulted to greater PCE efficiency (7.34%) mainly due to the complementary light absorption characteristics of the two dyes. Furthermore, the absorption features after co-sensitization suggests that compound **5** changed the orientation of the absorbed porphyrin molecules on TiO_2 and consequently decreased the aggregation. The co-sensitized solar cell exhibited enhanced electron injection efficiency and the Incident Photon to Current Efficiency (IPCE) spectrum has been broadened over the 350-700 nm range. In perfect agreement with the latter, the improved performance of the co-sensitized solar cell is also observed from enhancement of the J_{sc} curve (from 10.85 to 14.74 mA/cm^2).

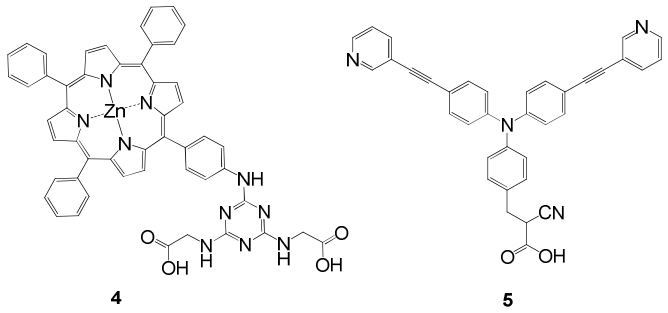

Fig. 5 Porphyrin **4** and tertiary aryl amine compound **5**.

In another approach, we wanted to examine if different metallated porphyrins with transition metals and four carboxylic acids as anchoring groups influence the performance of DSSC. Therefore, we synthesized a series of *meso*-carboxyphenyl porphyrins metallated with transitions metals (Pt, Pd, Rh and Ru) **6**–**9** were synthesised as sensitizers in DSSCs (Fig. 6).[61] The maximum conversion efficiency 0.13% was reported for compound **6**. The poor photovoltaic performance for all dyes is mainly attributed to unsuitable energy levels of Lowest Unoccupied Molecular Orbitals (LUMOs) of all porphyrin compounds. In addition, the long alkoxy chains (C_4) prevent aggregation, but lack conjugation resulting to low PCE values. The development of noble metallated porphyrin moieties with a higher LUMO level and conjugated long chains could improve the DSSC performance of such dyes and lead to greater PCE values. Therefore, the

presence of Ru, Rh, Pd and Pt metals on the porphyrin ring reduces the efficiency of the cell.

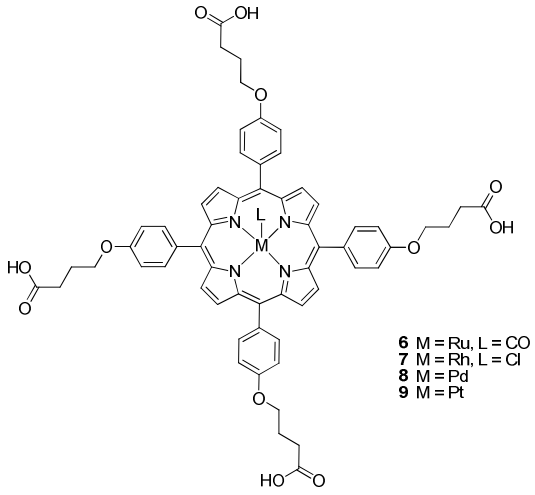

Fig. 6 Structures of porphyrin complexes **6–9**.

2.1.2 Covalently linked dimeric chromophores

Another effective approach to enhance the overall photovoltaic performance of porphyrin based solar cells is to employ as sensitizers covalently linked arrays of porphyrins. Porphyrin dimers and trimers are ideal potential photosensitizer candidates due to some specific properties that possess, such as their increased wavelength absorption and their extended conjugation of the porphyrin π-system. In addition, the type of the linkage between the porphyrin moieties can influence their structure and their electronic characteristics. The efficient electronic communication between the porphyrin arrays, in terms of intra- and/or inter-molecular charge transfer, is another key asset that marks those compounds as attractive not only for photovoltaic applications but also for Organic Light Emitting Diodes[62] and Photo Dynamic Therapy[63, 64] applications. The main drawback such porphyrin derivatives have, is the enhanced aggregation issues and their difficult, not straight forward synthesis.

Porphyrin arrays covalently linked either through π-conjugated bridges[65] or directly,[66] exhibit strong electronic coupling between porphyrin units, resulting in splitting of the Soret band and broadening of the Q-bands. Because of these spectral features, porphyrin arrays display improved overall harvesting

efficiencies, and lead to better photovoltaic performances relative to the corresponding monomeric porphyrin sensitizers.[65]

Therefore, we synthesized a series of covalently linked porphyrin dyads **10**–**15** (Fig. 7), in which the two porphyrin rings are covalently linked through the unit of *s*-triazine.[67-69] Cyanuric chloride was chosen as the bridging ligand, because its reactivity is temperature dependent and allows the introduction of up to three different nucleophiles on an *s*-triazine unit through sequential substitution of its three chlorine atoms. As a result, it is possible to use one-pot protocol reactions, providing a modular synthetic route to the desired multiporphyrin arrays in good yields and avoiding extensive and expensive preparative and purification procedures.

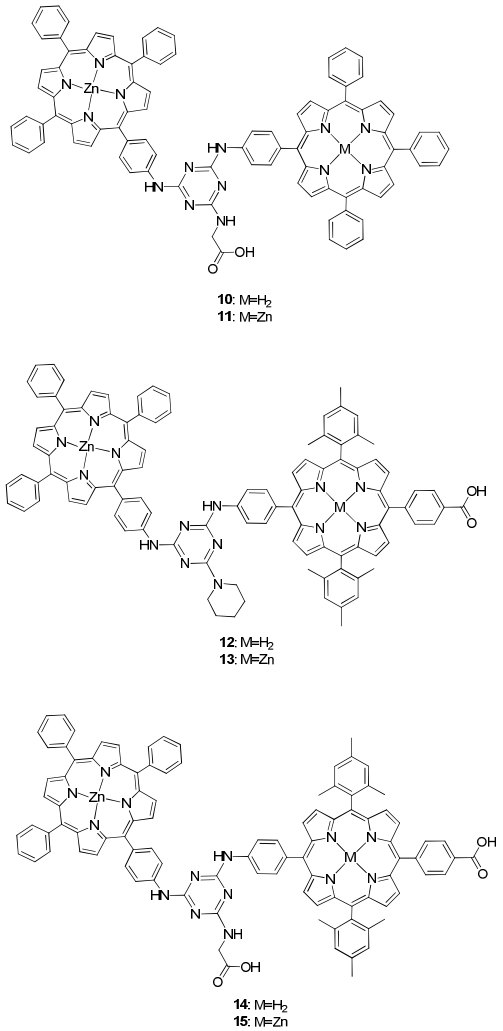

Fig. 7 Chemical structures of porphyrin dimers **10**–**15**.

By taking advantage of these properties we prepared dimers **10**–**15**. These dimers can be divided in two groups: the unsymmetrical (**10**, **12**, **14**) where only one of the two porphyin rings is metallated with zinc and the symmetrical (**11**, **13**, **15**) where both porphyrins contain zinc. Moreover, dimers **10**–**13** bear only one carboxylic acid as anchoring group, while compounds **14** and **15** have two anchoring groups. Absorption spectroscopy studies in solution were performed for all the synthesized dimers, and suggested that there is negligible intramolecular electronic interaction between the two porphyrins in their ground state. The electrochemical properties of porphyrin dyads **10**–**15** were investigated by cyclic voltammetry measurements. From the first oxidation potential and the first reduction potential we calculated the energies of their HOMO and LUMO molecular orbitals, respectively. These data in combination with DFT calculations revealed that all the dyads have suitable frontier orbital energy levels for use as sensitizers in DSSCs.

Solar cells sensitized by dyads **10**–**15** have been fabricated and their photovoltaic parameters are summarized in table 1. The **10** and **11** sensitized solar cells were found to exhibit PCE values of 4.46% and 3.61%, respectively. The superior performance of **10** is attributed to its unsymmetrical structure. The presence of a free-base and a zinc-metallated porphyin in **10** might cause a polarizing and cooperating effect that directs the electron transfer to the TiO_2 CB, and leads to more efficient electron injection, while in the symmetrical **11** there is no directionality in the electron transfer process. The same trend was also observed in the other dyads where the unsymmetrical dimers **12** and **14** exhibit higher PCE values compared to their corresponding symmetrical dyads **13** and **15**, respectively. However, the **10** based solar cell is not as efficient as the multiporphyrin arrays with the ‘‘push–pull’’ architecture, which exhibit PCE values over 5%.[65] This is ascribed to the fact that in **10** the carboxylic acid anchoring group resides on the triazine linker, while in ‘‘push–pull’’ systems it is located on the electron acceptor unit and, hence, results in very efficient charge transfer directionality and enhanced photocurrent.

For this reason we prepared dimers **12** and **13** (Fig. 7) where the anchoring group is located on one *meso*-phenyl ring of one porphyrin and not on

the *s*-triazine linker. Nevertheless, comparison of the PCE values of **12** with **10** showed that the position of the carboxylic acid does not alter significantly the efficiency of the prepared DSSCs. Moreover, dimers **11** and **13** also exhibit similar PCE values supporting the fact that the position of the anchoring group, in this family of compounds, is not affecting the electron transfer efficiency.

Finally we prepared dimers **14** and **15**, which bear two carboxylic acids, in order to examine the influence of the number of the anchoring groups in the PCE of the fabricated DSSCs. Comparison of the solar cells based on **15** and **13** revealed enhanced photovoltaic parameters and PCE value for the former (5.28% versus 3.50%, respectively). Apparently, the presence of two carboxylic acids in the molecular structure of **15**, results in a more effective binding onto the TiO_2 surface and, therefore, in the formation of a more compact dye layer on the TiO_2 surface, which is manifested by the increased dye loading of the **15** sensitized solar cell. Furthermore, it produces a cooperative effect in the electron transfer into the TiO_2 CB, which gives a faster and more efficient electron injection process. This is evidenced by EIS measurements revealing longer electron lifetime, and more effective suppression of charge recombination for the **15** based solar cell.

Table 1 Photovoltaic parameters under global AM 1.5 irradiation of the fabricated DSSCs using dimers **10–15**.

Dimer	J_{SC}[a], mA/cm^2	V_{OC}[b], V	FF[c]	PCE[d], %
10	9.94	0.66	0.68	4.46
11	8.82	0.63	0.65	3.61
12	9.84	0.62	0.68	4.15
13	8.56	0.62	0.63	3.50
14	11.44	0.68	0.70	5.44
15	10.78	0.68	0.72	5.28

[a]Short circuit current, [b]open circuit voltage, [c]fill factor, [d]power conversion efficiency.

An alternative approach for extending the light harvesting efficiency of DSSCs involves the co-sensitization of the TiO_2 film with two or more molecular sensitizers that exhibit strong and complementary absorption profiles. Based on this idea, we used dyad **10** (Fig. 7) and a tertiary arylamine compound **16** (Fig. 8),

which contains a terminal cyano-acetic group in one of its aryl groups, for the construction of co-sensitized DSSCs.[70] For the fabrication of the cells, a stepwise co-sensitization procedure was followed, by sequentially immersing the TiO_2 electrode in separate solutions of **10** and **16** dyes. For comparison purposes, solar cells sensitized by the individual dyes **10** and **16**, were also fabricated, under the same experimental conditions. The individually sensitized devices **10** and **16** were found to exhibit PCE values of 4.46%, and 4.45%, respectively, while the co-sensitized solar cell device showed PCE value of 6.16%. The higher PCE value of the co-sensitized device was attributed to enhanced light harvesting efficiency (LHE). Absorption spectroscopy studies showed that the co-sensitized film exhibits very strong absorption in the 460–530 nm range, where the absorption of the **10** sensitized film is weak. Hence, the absorption spectrum of the **10**/**16** film exhibits an extended absorption profile with panchromatic features, which leads to an increased LHE.

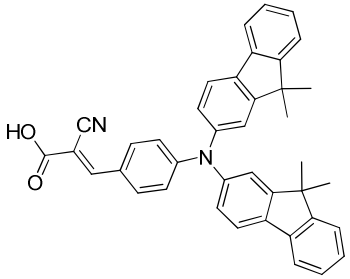

16

Fig. 8 Chemical structure of metal free organic dye **16**.

The PCE of the **10**/**16** co-sensitized device was further improved up to 7.68% when a formic acid treated TiO_2 photoanode was used. This enhancement was attributed to the higher J_{sc} and V_{oc} values, due to modification of the electronic properties of the TiO_2 CB. Dark current and EIS measurements revealed an increased electron transport rate and suppressed electron recombination in the formic acid treated TiO_2 photoanode.

Continuing our study on dimeric dyes we prepared two porhyrins connected with two different bridges in order to examine whether the length can influence the performance of the cell. Therefore, we synthesized dyads **17** and **18** (Fig. 9) consisting of two zinc-metallated porphyrin units, which are covalently

linked through their *meso*-phenyl groups by 1,2,3-triazole ring.[71] These dimers were synthesized via "click" reactions, which are Cu-catalyzed Huisgen 1,3-dipolar cycloadditions between azide and acetylene-containing porphyrins. UV-vis spectra and cyclic voltammetry measurements, as well as DFT calculations, revealed that there is negligible electronic interaction between the two porphyrin units in the ground states of both dyads, but the dyads possess frontier orbital energy levels which are suitable for use as sensitizers in DSSCs. Fabrication of the corresponding solar cells revealed that the device based on the dyad **18** with the shorter bridge results in a better photovoltaic performance. The PCE values for the **17** and **18** based solar cells were measured 3.82% and 5.16%, respectively. The higher PCE value of the latter was attributed to its enhanced short circuit current (J_{sc}) under illumination, its longer electron lifetime (τ_e) and more effective charge recombination resistance between the injected electrons and the electrolyte, as well as its higher dye loading on the TiO_2 surface. Comparison of the PCE values of dimeric compounds **11**, **13**, **17** and **18** where both porphyrin rings are metallated with zinc and contain one anchoring group showed that dimer **18** had the highest efficiency. Therefore, the presence of the triazole ring with the short aliphatic chain between the two porphyrin rings enhances the performance of the device.

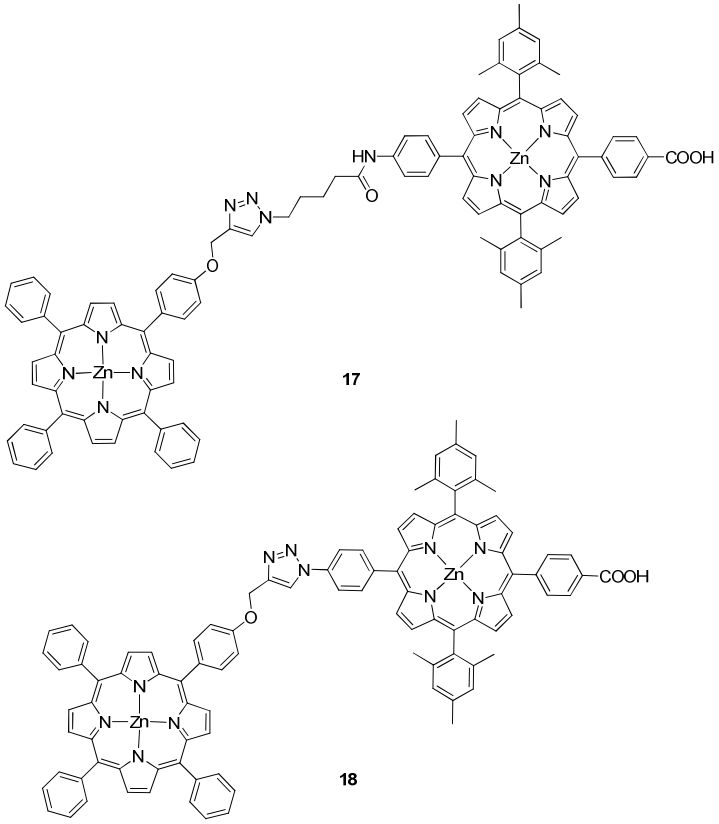

Fig. 9 Chemical structures of porphyrin dimers **17** and **18**.

2.1.3 Covalently linked trimeric chromophores

In line with our research interest on developing improved porphyrin complexes for DSSC applications, we developed further our findings on dimeric dyad **12** by replacing the piperidine molecule with a zinc porphyrin. The extra porphyrin was added in order to enhance the light harvesting efficiency of the prepared DSSCs. In the course of this study we synthesized a triazine-linked porphyrin triad **19** (Fig. 10) consisting of two zinc-metallated porphyrins and one free-base porphyrin bearing a carboxylate group.[72] Trimeric compound **19** can be described as a "push-pull" 2D-π-A system (D: donor, π: conjugated system and A: acceptor). The donor units, namely the zinc-metallated porphyrins, promote the intramolecular electron transfer through the π-conjugated system (triazine) to the acceptor free-base porphyrin, which contains the carboxylic acid for efficient attachment on TiO_2. In this work, two different types of photoanodes have been used, with respect of the fabrication method that has been applied. The

photoanodes were processed either by paste-coating (PC) method or by electrophoretic deposition (EPD) method, leading to PCE values of 3.80% and 4.91% respectively. These values are comparable with those observed for dimer **12**. Therefore the presence of a third porphyrin ring does not improve the efficiency. The reported enhanced value of EPD method was correlated with the surface morphology and electron-transport kinetics. The EIS spectra revealed that EPD-processed photoanode exhibits longer electron lifetime, higher charge recombination resistance and shorter electron-transport time, comparing to the PC-processed photoanode. In addition, further improvement of EPD-processed photoanode was achieved (5.56%) through co-sensitization of CDCA in the dye solution.

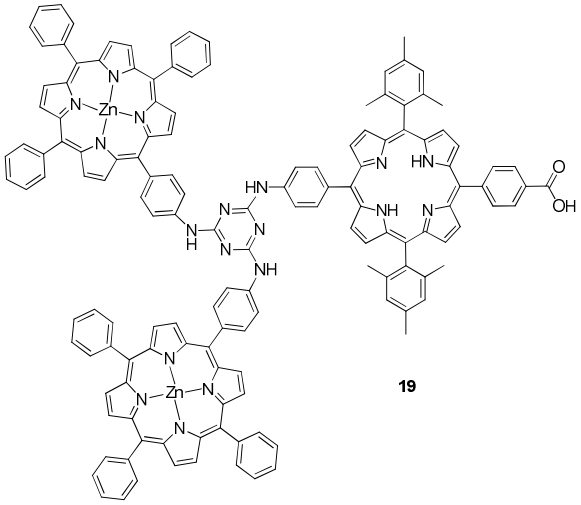

19

Fig. 10 Chemical structure of porphyrin trimer **19**.

In order to understand if the presence of two anchoring groups on the porphyrin trimeric compounds influences the performance of the cell, another compound **20** was synthesized using two triazine moieties as bridges.[74] In trimer **20** (Fig. 11) the central zinc-metallated porphyrin is connected through triazine groups with two free-base porphyrin units. Each peripheral free-base porphyrin contain carboxylic acid that act as anchoring group to TiO_2 nanoparticles. Porphyrin **20** can be described as a "push-pull" D-π-2A system, with the terminal free-base porphyrin as acceptor units, the zinc-porphyrin unit as the donor group and π denoting the triazine bridge. The photovoltaic measurements revealed a

PCE value of 5.88% using CDCA as co-adsorbent. In addition, the DSSC sensitized with **20** exhibits high short circuit current (J_{sc} = 12.18 mA/cm^2) and open circuit voltage (V_{oc} = 0.68 V). The high PCE value is correlated with the EIS studies, specifically the long electron life-time and short electron transport time that we observed in the case of **20**. Moreover, the EIS studies showed suppressed electron recombination and reduced dark current, aspects crucial for the reported DSSC performance. By comparison of the PCE values of trimeric porphyrins **19** and **20**, it is concluded that the addition of an extra anchoring group (compound **20**) does not significantly affect the performance of the cell.

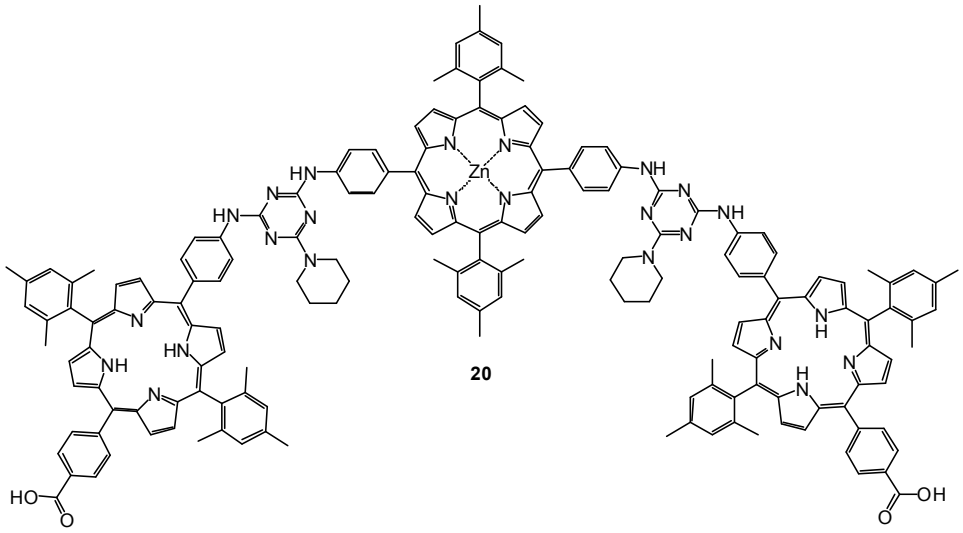

Fig. 11 Chemical structure of triazine-linked trimer **20**.

In order to extend the light absorption of porphyrin-based sensitizers to even wider spectral regions, we combined porphyrins with other types of chromophores, as additional antenna components. Based on the encouraging results of trimer **19** we replaced the two zinc porphyrins with a different chromophore such as 4,4-difluoro-4-bora-3a,4a-diaza-s-indacene (BODIPY), preparing a BODIPY-porphyrin triad **21** (Fig. 12).[73] The compound was synthesized via stepwise amination reactions where a carboxyphenyl *meso*-substituted porphyrin was covalently attached with two BODIPY molecules via 1,3,5-triazine bridge. In this triad the BODIPY molecules act as an antenna and after their excitation an efficient energy transfer from the BODIPY to the porphyrin takes place. For the preparation of the DSSCs, various immersion times of the TiO_2

electrode into the solution of the porphyrin were investigated and it was found that 4 h was the ideal time regarding the photovoltaic performance of the device. Solar cells sensitized by trimer **21** exhibit a PCE value of 5.17% which is improved compared to trimer **19** (3.80%). Therefore, the presence of BODIPY molecules further increases the PCE values. Additionally, incorporation of reduced graphene oxide (rGO) between TiO_2 and dye **21** resulted the formation of rGO-TiO_2 barrier in the device with an improved efficiency (6.20%) along with higher J_{sc} and fill factor (FF) values. The barrier that is formed, assist the electron transport process towards the FTO surface more efficiently as the EIS studies suggest. More precisely, the rGO-TiO_2 photoelectrode exhibit shorter transport time, longer electron time and lower charge transfer resistance.

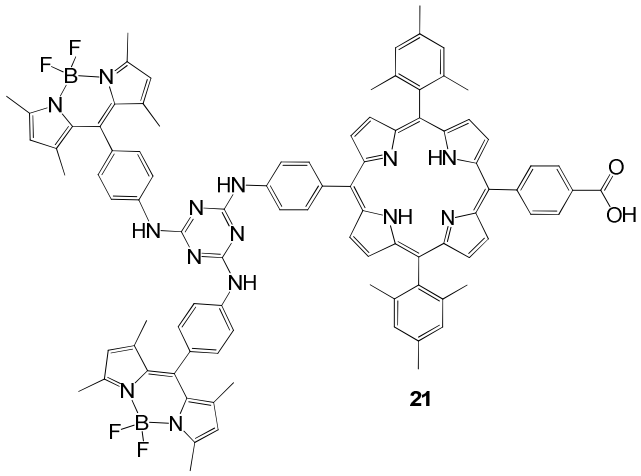

21

Fig. 12 Structure of BODIPY-porphyrin triad **21**.

In addition, we synthesized triads **22** and **23** (Fig. 13) in which two $[Ru(bipy)_3]^{2+}$ (bipy = 2,2'-bipyridine) units and two BODIPY are linked to a porphyrin unit, respectively.[75] In compound **22** the two $Ru(bipy)_3$ chromophores are linked through amide bonds to the peripheral aryl groups of a free-base porphyrin unit. While in triad **23**, two BODIPY moieties are connected through ethynyl groups at opposite *meso*-positions of a zinc metallated porphyrin. Both triads exhibit UV–Vis absorption spectra with absorption features of their constituent chromophores, and hence wider spectral absorptions than the corresponding porphyrins. Emission studies in **22** revealed that the two chromophores interact only weakly in their excited state. The PCE value for the

22 based solar cell was 0.3%. As suggested by DFT calculations, the low performance was attributed to the unsuitable positioning of the frontier molecular orbitals of the triad, since its LUMO electronic density is primarily localized over the two $[Ru(bipy)_3]^{2+}$ units, and not on the carboxylic acid anchoring groups, as it should be expected for efficient electron injection into the TiO_2 CB. On the other hand, combination of steady-state and time resolved emission spectra of trimer **23** clearly showed photoinduced energy transfer from the $^1\pi$–π* excited state of the BODIPY chromophore to the lower lying singlet excited state of the porphyrin unit, leading to sensitized fluorescence from the latter. However, despite the efficient energy transfer the PCE of the **23** based solar cell was 0.6%.

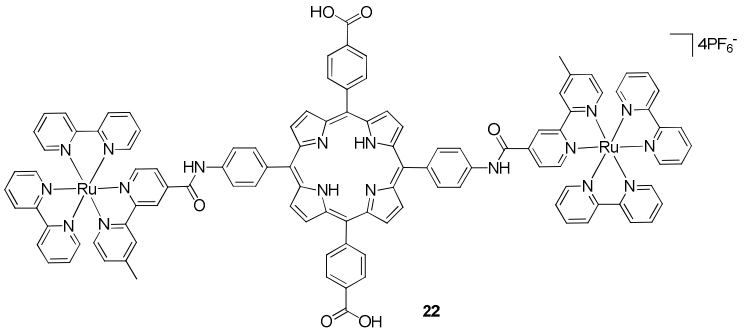

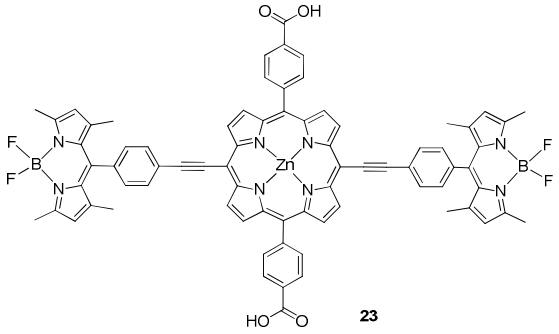

Fig. 13 Chemical structures of porphyrin trimmers **22** and **23**.

2.2 Porphyrins for DSSC with pyridyl anchoring groups

As mentioned so far, most of the dyes reported in the literature possess one or more carboxylic acids as anchoring groups for their attachment on a TiO_2 surface. On the other hand quite recently a pyridine ring is used as an electron withdrawing anchoring group.[76, 77] These dyes were found to give better electron injection efficiencies compared to the corresponding porphyrins bearing

carboxylic acids as anchoring groups.[76-78] This was attributed to the nature of the coordinate bond between pyridine and the Lewis acid sites of the TiO_2 surface, which provides better electronic communication than the ester linkage of the carboxylic acid groups. In order to investigate the performance of sensitizers having pyridyl ring as anchoring group we synthesized a series of *meso* substituted porphyrins **24**–**26** which bear one, two and four pyridyl groups (Fig. 14).[79]

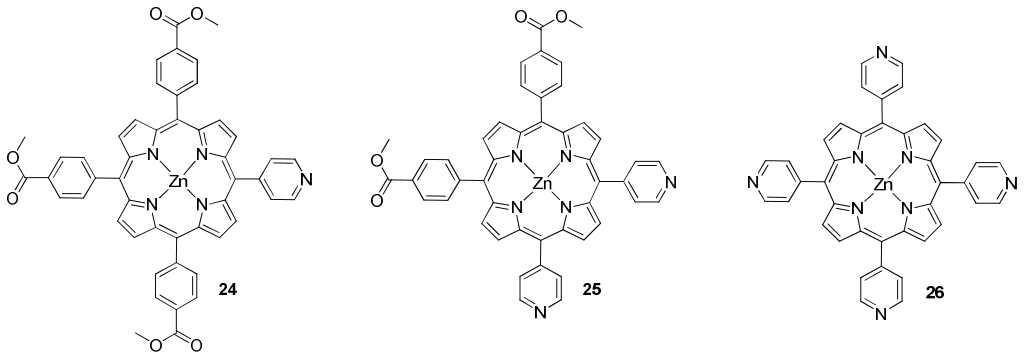

Fig. 14 Porpyrin dyes **24**–**26** with *meso* substituted pyridyl anchoring groups.

The overall power conversion efficiencies of DSSCs based on these dyes are 3.10%, 3.90% and 2.46%, for the **24**, **25** and **26** respectively. The highest photovoltaic parameters and PCE value obtained for the porphyrin derivative with two pyridyl groups, **25** (3.90%). This can be attributed to the high dye loading, efficient electron injection, dye regeneration process and longer electron lifetime as measured by the EIS. Even though the PCE of **25** is the highest among the three porphyrins is low compared to other porphyrin dyes reported in the literature.[35, 80, 81] When the photoanode of the **25**-sensitized solar cell was treated with formic acid higher amount of dye adsorbed onto TiO_2 yielded an increased PCE value of 5.24%. Moreover, DCA was used as coadsorbant for dye **25** in order to prevent dye aggregation and an improved PCE of 6.12% was measured that was attributed to further improvement in the electron injection efficiency and charge collection efficiency.

The performance of dye **25** was additionally increased by co-sensitization with a mononuclear ruthenium(II) complex **27** (Fig. 15), giving a PCE value of

7.35%.[82] In addition, the efficiency of this co-sensitized solar cell was further improved up to 8.15% using a graphene modified TiO_2 photoanode, instead of a pure TiO_2 photoanode. The increased PCE value of the graphene modified photoanode solar cell as suggested by dark current measurements and EIS, can be attributed to the suppression of charge recombination at the photoanode/dye/electrolyte interface and enhancement of electron transfer between the photoanode and the collecting electrode.

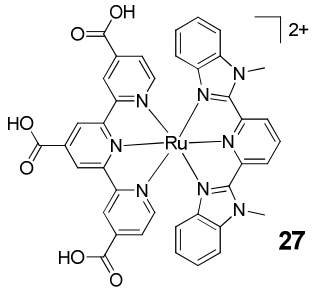

27

Fig. 15 Mononuclear ruthenium(II) complex **27**.

In order to improve the promising results that were obtained with the use of pyridyl as anchoring group, we prepared porphyrin dye **28** with a pyridyl group connected through a triple bond to the aromatic porphyrin core (Fig. 16).[83] The overall power conversion efficiency of DSCC based on porphyrin **28** was 3.36%. This value is similar to the one measured for porphyrin **24**, so the introduction of a triple bond between the pyridyl and the porphyrin ring does not affect significantly the PCE value. The low reported efficiency for porphyrin **28** is due to dye aggregation upon coordination on TiO_2. The use of a CDCA as a coadsorbant reduced the aggregation and improved the solar cell efficiency up to 4.56%. Moreover, when Ag nanoparticles were incorporated into the photoanode, the efficiency of the cell was increased up to 5.66%. This enhancement was attributed to the increased light harvesting efficiency in the visible region of the solar spectrum, and hence its short circuit current density. Also, the charge transport and electron lifetime were improved.

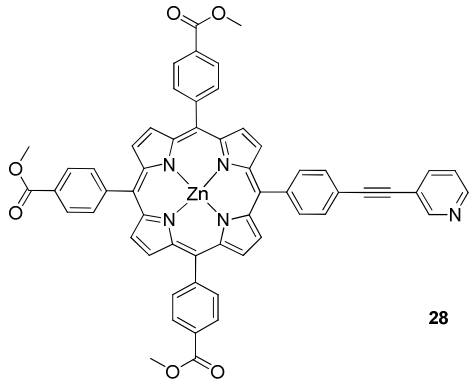

28

Fig. 16 Chemical structure of tricarboxy-pyridinylethynyl porphyrin dye **28**.

It is known that the electrolyte additives used in DSSCs can affect their performance. They can change the short circuit current and the open circuit voltage, by shifting positively or negatively the TiO_2 CB edge. Also they can alter the recombination kinetics at the TiO_2/electrolyte interface.[84] The compounds that have been used as electrolyte additives in the DSSCs are 4-tert-butylpyridine, 4-methylbenzimidazole, guanidinium thiocyanate, and thiourea.[85, 86] Therefore, during our studies thiourea containing electrolyte was used and the PCE value of porphyrin **28** was increased to 5.34%.[87] The enhancement of the solar cell efficiency was attributed to an increase of the short circuit current density, which was due to a positive shift of the TiO_2 conduction band edge, and to a decrease in the charge recombination rate. UV–Vis absorption spectra and X-ray powder diffraction patterns of pure and thiourea-containing TiO_2 films also suggested that thiourea molecules are chemisorbed onto TiO_2, and passivize its surface recombination sites between the injected electrons and the I_3^- ions of the electrolyte. The resulting slower recombination kinetics (which is documented by a longer electron lifetime) is also suggested to as a reason for the slight increase of the open circuit voltage of the solar cell, which compensates for the opposing effect of the positive shift of the TiO_2 CB edge.

Moreover, in order to extend our studies on porphyrin dyes bearing pyridyl anchoring groups, we synthesized a free-base *meso*-tetraaryl porphyrin **29** and its zinc analogue **30** (Fig. 17).[88] These compounds are having four oligo(p-phenylenevinylene) (oPPV) pyridyl groups with long dodecyloxy chains on the phenyl groups. The presence of the long alkoxy chains on the *meso*-phenyl

groups offers the advantage of high solubility in a variety of organic solvents; also they could prevent porphyrin aggregation. The PCE values were measured for free-base **29** and zinc porphyrin **30** 3.28% and 5.12%, respectively. The higher PCE value of metallated porphyrin **30** was ascribed to higher short-circuit current, open-circuit voltage, and dye loading values.

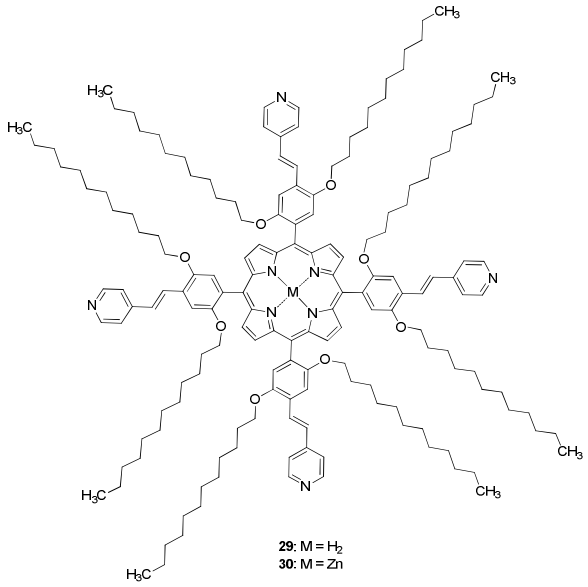

Fig. 17 Chemical structures of porphyrins **29** and **30**.

Table 2 summarizes the photovoltaic parameters (J_{SC}, V_{OC} and FF) as well as the PCE values for all the porphyrin dyes with pyridyl anchoring groups, prepared from our team. In the case of the mono substituted pyridyl compounds **24** and **28** that differ in the length and the position of the nitrogen atom (*para vs meta* position) the PCE values were quite similar (~3.2%). Regarding tetra pyridyl porphyrins, there was an increase from 2.46% (**25**) to 5.12% (**30**). The enhanced photovoltaic properties of **30** may be attributed to the long alkoxy chains that prevent the aggregation. While in the case of **25**, possibly the formation of porphyrin-porphyrin aggregates that occurs through zinc metal-pyridine coordination may hinder the attachment on TiO_2 surface.

Table 2 Photovoltaic parameters of the fabricated DSSCs using porphyrin dyes with pyridyl anchoring groups **24-26** and **28-30**.

Dye	J_{SC}[a], mA/cm^2	V_{OC}[b], V	FF[c]	PCE[d], %

24	9.2	0.60	0.56	3.10
25	10.56	0.64	0.60	3.90
26	7.6	0.60	0.54	2.46
28	9.38	0.64	0.56	3.36
29	8.86	0.64	0.58	3.28
30	11.25	0.68	0.67	5.12

[a]Short circuit current, [b]open circuit voltage, [c]fill factor, [d]power conversion efficiency.

3. Porphyrins for BHJ

In BHJ organic cells the absorber active layer is a blend of donor and acceptor molecules. As electron donor materials are usually used conjugated polymers or conjugated pigments and as acceptors fullerene derivatives.[89-98] Despite the high PCEs achieved for polymer BHJ solar cells, the application of these solar cells for commercial applications is limited due to their low reproducibility for characteristics such as average molecular weight and polydispersity index as well as difficulty in purification. Therefore, in the place of polymers, small molecules have been prepared and used as electron donor materials with efficiencies up to 6-7%, close to their polymer-base counterparts.[99-105] These small molecules exhibit several advantages such as definite molecular weight and high purity without batch to batch variations, versatile molecular structure and easier band structure control. The organic solar cells fabricated with vacuum processed small molecules showed PCEs of 6.4% and 10.7% for a single layer BHJ solar cell and multi-layered tandem solar cell, respectively.[106, 107] The most important key factor for high PCE in BHJ layer is the donor materials. The donor molecules should exhibit a strong and a wide range absorption profile. They must also display certain properties such as sufficient solubility in common organic solvents, ability to form strong intermolecular interactions in the solid state for efficient charge transfer, conduction band edge higher than that of the acceptor material, and high light- and air-stability.

The interest of using porphyrins as donor materials in BHJ organic solar cell is attributed to their very well established role as light harvesting antenna for efficient energy and electron transfer processes in biological systems.[108-113] Porphyrin molecules also exhibit many interesting properties as discussed in

section 2, making them suitable for applications as donors for vacuum deposited organic solar cells[114] and as light absorbing dyes in DSSCs.[3, 49] Despite the successful employment of porphyrins as sensitizers in DSSCs their utilization as donors in solution-processed BHJ organic solar cells has been rather limited.[115-119]

Therefore, porphyrin molecules that were used as dyes in DSSCs in our group were also examined in BHJ organic solar cells. More specifically, the compounds that examined were monomeric compound **28**, dimeric dye **13** and trimeric chromophores **19** and **21**. All porphyrin examples in this section were used as electron donors and different fullerene compounds as electron acceptors. All the combinations of the active layers that were prepared along with their measured PCE values are summarized in table 3. In one case porphyrin derivative **28** (Fig. 16) was used as an electron donor and a fullerene [6,6]-phenyl C_{60} butyric acid methyl ester (**$PC_{60}BM$**) or [6,6]-phenyl C_{70} butyric acid methyl ester (**$PC_{70}BM$**) as an electron acceptor (Fig. 18).[120] The BHJ organic solar cell based on porphyrin **28**:**$PC_{60}BM$** and **28**:**$PC_{70}BM$** exhibited a PCE of 1.96% and 2.54%, respectively. The higher PCE of **$PC_{70}BM$** is attributed to the higher value of J_{sc} that is related to its strong absorption in the visible region compared to **$PC_{60}BM$**. In the case of **$PC_{70}BM$** the PCE was further improved to 3.27% when thermally annealed **28**:**$PC_{70}BM$** was used as active layer. This enhancement is related to the increase value of holes mobility upon thermal annealing that leads to more balanced charge transport in the device. Moreover, the PCE of the device of **28**:**$PC_{70}BM$** was further improved up to 4.06% when a modified PEDOT:PSS DMF treated buffer layer was used.

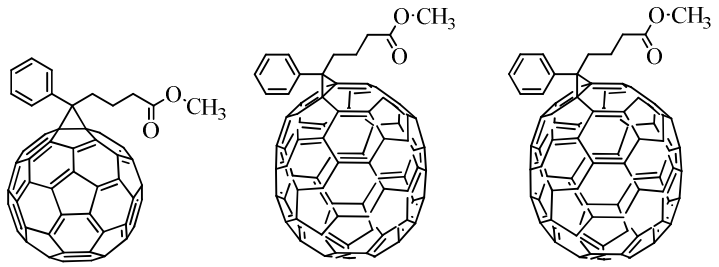

$PC_{60}BM$ **$PC_{70}BM$** **$PC_{71}BM$**

Fig. 18 Chemical structure of **$PC_{60}BM$**, **$PC_{70}BM$** and **$PC_{71}BM$** molecules.

In the following examples BHJ organic solar cells were prepared in THF based on a blend of 1:1 weight ratio using porphyrins **13** (Fig. 7), **21** (Fig. 12) and **19** (Fig. 10) as electron donors and as electron acceptors **$PC_{70}BM$** and **$PC_{71}BM$** (Fig. 18). The active layers **13**:**$PC_{71}BM$**,[121] **21**:**$PC_{71}BM$** [122] and **19**:**$PC_{70}BM$** [123] resulted PCEs of 2.91%, 3.48% and 2.85%, respectively (Table 3). In an effort to improve the solar cell efficiency the active layer was treated with a pyridine in THF mixture of 3% v/v in the case of **13**:**$PC_{71}BM$** and 4% v/v in the case of **21**:**$PC_{71}BM$**. In both cases the PCE values were increased to 4.16% and 5.29%, respectively. This was ascribed to an enhancement of the short circuit current J_{sc} of the solar cell, which is related to the different surface morphology of the active layer blend upon pyridine addition. The pyridine-modified active layer exhibited a higher degree of crystallinity resulting in an increase of exciton dissociation efficiency and more balanced charge transport. Moreover, in the case of **19**:**$PC_{70}BM$** the efficiency was improved to 3.93% when the active layer was processed with a 5% v/v solvent mixture of 1-chlotonaphthalene in THF. This increase was again due to the higher degree of crystallinity of the active layer of the latter solar cell.

Table 3. PCE measurements of BHJ Organic solar cells based on differently processed active layers of Electron donor:Electron acceptor in 1:1 weight ratio.

Electron Donor	Electron Acceptor	PCE, %
28	**$PC_{60}BM$**	1.96
28	**$PC_{70}BM$**	2.54
		4.06[a]
13	**$PC_{71}BM$**	2.91
		4.16[b]
21	**$PC_{71}BM$**	3.48
		5.29[c]
19	**$PC_{70}BM$**	2.85
		3.93[d]

[a]Treated with PEDOT:PSS buffer layer, [b]Treated with 3% v/v pyridine in THF, [c]Treated with 4% v/v of pyridine in THF, [d]Treated with 5% v/v of 1-chloronaphtalene in THF.

4. Conclusions

In this review we present various porphyrin molecules synthesized in our group and used as chromophores for DSSC and BHJ applications. In the case of DSSC devices monomeric, dimeric and trimeric dyes were used either on their own or with co-sensitization of the TiO_2 film with small organic molecules that exhibit strong and complementary absorption profiles. In all cases co-adsorption increased the PCE values of the chromophores possibly due to enhanced light harvesting efficiency and/or to decreased dye aggregation. Moreover, zinc metallated porphyrins exhibit higher PCE values compared to their free-base counterparts. When dimeric compounds were used as dyes, where only one of the porphyrin rings is metallated with zinc and the other is non metallated, exhibited better performances compared to their fully metallated counterparts. This enhancement may be attributed to the polarizing and cooperating effect that directs the electron transfer to the TiO_2 CB therefore, leading to more efficient electron injection. In dyes bearing carboxylic groups the position of the anchoring group does not alter significantly the efficiency of the prepared DSSCs. Dyes with two carboxylic acids bind more efficient onto the TiO_2 surface increasing the performance of the cell. The same trend was also observed when a pyridyl ring was used as anchoring group. The best PCE values were obtained in the case of porphyrins with four pyridyl groups and with long alkyl chains preventing aggregation. Moreover, various porphyrins were synthesized and used as electron donor materials in BHJ organic solar cells. The best efficiency obtained when a trimeric compound was used consisting of two BODIPY and one porphyrin molecule as a donor and a fullerene as an electron acceptor (**21:PC_{71}BM**).

5. Acknowledgments

Financial support from the European Commission (FP7-REGPOT-2008-1, Project BIOSOLENUTI No. 229927) is greatly acknowledged, as well Special Research Account from the University of Crete.

6. References

1. S. W. Glunz, *Adv. OptoElectron.*, 2007, **2007**, 15.

2. C. J. Brabec, V. Dyakonov and U. Scherf, *Materials Device Physics and Manufacturing Technologies*, Wiley-VCH, Weinheim, 2008.
3. S. Mathew, A. Yella, P. Gao, R. Humphry-Baker, B. F. E. Curchod, N. Ashari-Astani, I. Tavernelli, U. Rothlisberger, M. K. Nazeeruddin and M. Gratzel, *Nature Chemistry*, 2014, **6**, 242-247.
4. S. E. Shaheen, C. J. Brabec, N. S. Sariciftci, F. Padinger, T. Fromherz and J. C. Hummelen, *Appl. Phys. Lett.*, 2001, **78**, 841-843.
5. M. A. Green, K. Emery, Y. Hishikawa, W. Warta and E. D. Dunlop, *Prog. Photovoltaics*, 2012, **20**, 12-20.
6. B. Oregan and M. Gratzel, *Nature*, 1991, **353**, 737-740.
7. M. Kivala and F. Diederich, *Acc. Chem. Res.*, 2009, **42**, 235-248.
8. S.-i. Kato and F. Diederich, *Chem. Commun.*, 2010, **46**, 1994-2006.
9. H. Meier, *Angew. Chem. Int. Edit.*, 2005, **44**, 2482-2506.
10. M. Kivala and F. Diedericht, *Pure Appl. Chem.*, 2008, **80**, 411-427.
11. A. Cravino, S. Roquet, P. Leriche, O. Aleveque, P. Frere and J. Roncali, *Chem. Commun.*, 2006, 1416-1418.
12. S. Tao, Y. C. Zhou, C. S. Lee, S. T. Lee, D. Huang and X. H. Zhang, *J. Phys. Chem. C*, 2008, **112**, 14603-14606.
13. K. Hara, Y. Tachibana, Y. Ohga, A. Shinpo, S. Suga, K. Sayama, H. Sugihara and H. Arakawa, *Sol. Energy Mater. Sol. Cells*, 2003, **77**, 89-103.
14. K. Hara, T. Sato, R. Katoh, A. Furube, Y. Ohga, A. Shinpo, S. Suga, K. Sayama, H. Sugihara and H. Arakawa, *J. Phys. Chem. B*, 2003, **107**, 597-606.
15. D. Kuang, S. Uchida, R. Humphry-Baker, S. M. Zakeeruddin and M. Gratzel, *Angew. Chem. Int. Edit.*, 2008, **47**, 1923-1927.
16. T. Horiuchi, H. Miura, K. Sumioka and S. Uchida, *J. Am. Chem. Soc.*, 2004, **126**, 12218-12219.
17. S. Kim, J. K. Lee, S. O. Kang, J. Ko, J. H. Yum, S. Fantacci, F. De Angelis, D. Di Censo, M. K. Nazeeruddin and M. Gratzel, *J. Am. Chem. Soc.*, 2006, **128**, 16701-16707.
18. H. Qin, S. Wenger, M. Xu, F. Gao, X. Jing, P. Wang, S. M. Zakeeruddin and M. Gratzel, *J. Am. Chem. Soc.*, 2008, **130**, 9202-9203.
19. P. Bonhote, J. E. Moser, R. Humphry-Baker, N. Vlachopoulos, S. M. Zakeeruddin, L. Walder and M. Gratzel, *J. Am. Chem. Soc.*, 1999, **121**, 1324-1336.
20. Y. Shirota, *J. Mater. Chem.*, 2000, **10**, 1-25.
21. G. L. Zhang, H. Bala, Y. M. Cheng, D. Shi, X. J. Lv, Q. J. Yu and P. Wang, *Chem. Commun.*, 2009, 2198-2200.
22. D. P. Hagberg, J. H. Yum, H. Lee, F. De Angelis, T. Marinado, K. M. Karlsson, R. Humphry-Baker, L. C. Sun, A. Hagfeldt, M. Gratzel and M. K. Nazeeruddin, *J. Am. Chem. Soc.*, 2008, **130**, 6259-6266.
23. H. N. Tian, X. C. Yang, J. Y. Cong, R. K. Chen, J. Liu, Y. Hao, A. Hagfeldt and L. C. Sun, *Chem. Commun.*, 2009, 6288-6290.
24. C. H. Chen, Y. C. Hsu, H. H. Chou, K. R. J. Thomas, J. T. Lin and C. P. Hsu, *Chem. - Eur. J.*, 2010, **16**, 3184-3193.
25. S. Hwang, J. H. Lee, C. Park, H. Lee, C. Kim, C. Park, M. H. Lee, W. Lee, J. Park, K. Kim, N. G. Park and C. Kim, *Chem. Commun.*, 2007, 4887-4889.
26. B. K. Spraul, S. Suresh, T. Sassa, M. A. Herranz, L. Echegoyen, T. Wada, D. Perahia and D. W. Smith, *Tetrahedron Lett.*, 2004, **45**, 3253-3256.
27. S. K. Lee, D. H. Hwang, B. J. Jung, N. S. Cho, J. Lee, J. D. Lee and H. K. Shim, *Adv. Funct. Mater.*, 2005, **15**, 1647-1655.
28. J. M. Raimundo, P. Blanchard, N. Gallego-Planas, N. Mercier, I. Ledoux-Rak, R. Hierle and J. Roncali, *J. Org. Chem.*, 2002, **67**, 205-218.

29. G. Yu, J. Gao, J. C. Hummelen, F. Wudl and A. J. Heeger, *Science*, 1995, **270**, 1789-1791.
30. C. Deibel and V. Dyakonov, *Rep. Prog. Phys.*, 2010, **73**.
31. A. J. Heeger, *Adv. Mater.*, 2014, **26**, 10-28.
32. M. K. Nazeeruddin, C. Klein, P. Liska and M. Gratzel, *Coord. Chem. Rev.*, 2005, **249**, 1460-1467.
33. A. Hagfeldt, G. Boschloo, L. C. Sun, L. Kloo and H. Pettersson, *Chem. Rev.*, 2010, **110**, 6595-6663.
34. C. P. Hsieh, H. P. Lu, C. L. Chiu, C. W. Lee, S. H. Chuang, C. L. Mai, W. N. Yen, S. J. Hsu, E. W. G. Diau and C. Y. Yeh, *J. Mater. Chem.*, 2010, **20**, 1127-1134.
35. T. Bessho, S. M. Zakeeruddin, C. Y. Yeh, E. W. G. Diau and M. Gratzel, *Angew. Chem. Int. Edit.*, 2010, **49**, 6646-6649.
36. H. S. He, A. Gurung and L. P. Si, *Chem. Commun.*, 2012, **48**, 5910-5912.
37. W. Zhou, Z. Cao, S. Jiang, H. Huang, L. Deng, Y. Liu, P. Shen, B. Zhao, S. Tan and X. Zhang, *Org. Electron.*, 2012, **13**, 560-569.
38. M. S. Kang, S. H. Kang, S. G. Kim, I. T. Choi, J. H. Ryu, M. J. Ju, D. Cho, J. Y. Lee and H. K. Kim, *Chem. Commun.*, 2012, **48**, 9349-9351.
39. C. Jiao, N. Zu, K.-W. Huang, P. Wang and J. Wu, *Org. Lett.*, 2011, **13**, 3652-3655.
40. C.-W. Lee, H.-P. Lu, C.-M. Lan, Y.-L. Huang, Y.-R. Liang, W.-N. Yen, Y.-C. Liu, Y.-S. Lin, E. W.-G. Diau and C.-Y. Yeh, *Chem. -Eur. J.*, 2009, **15**, 1403-1412.
41. M. K. Nazeeruddin, E. Baranoff and M. Grätzel, *Sol. Energy*, 2011, **85**, 1172-1178.
42. W. M. Campbell, A. K. Burrell, D. L. Officer and K. W. Jolley, *Coord. Chem. Rev.*, 2004, **248**, 1363-1379.
43. M. G. Walter, A. B. Rudine and C. C. Wamser, *J. Porphyrins Phthalocyanines*, 2010, **14**, 759-792.
44. L. L. Li and E. W. G. Diau, *Chem. Soc. Rev.*, 2013, **42**, 291-304.
45. M. K. Panda, K. Ladomenou and A. G. Coutsolelos, *Coord. Chem. Rev.*, 2012, **256**, 2601-2627.
46. P. A. Angaridis, T. Lazarides and A. C. Coutsolelos, *Polyhedron*, 2014, **82**, 19-32.
47. K. Ladomenou, T. N. Kitsopoulos, G. D. Sharma and A. G. Coutsolelos, *RSC Adv.*, 2014, **4**, 21379-21404.
48. A. G. Coutsolelos, K. Ladomenou, G. Charalambidis and D. Dafnomili, *The Porphyrin Handbook*, 2014.
49. A. Yella, C. L. Mai, S. M. Zakeeruddin, S. N. Chang, C. H. Hsieh, C. Y. Yeh and M. Gratzel, *Angew. Chem. Int. Edit.*, 2014, **53**, 2973-2977.
50. K. Murakoshi, G. Kano, Y. Wada, S. Yanagida, H. Miyazaki, M. Matsumoto and S. Murasawa, *J. Electroanal. Chem.*, 1995, **396**, 27-34.
51. J. N. Clifford, E. Palomares, M. K. Nazeeruddin, M. Gratzel, J. Nelson, X. Li, N. J. Long and J. R. Durrant, *J. Am. Chem. Soc.*, 2004, **126**, 5225-5233.
52. E. Palomares, M. V. Martinez-Diaz, S. A. Haque, T. Torres and J. R. Durrant, *Chem. Commun.*, 2004, 2112-2113.
53. J. R. Durrant, S. A. Haque and E. Palomares, *Coord. Chem. Rev.*, 2004, **248**, 1247-1257.
54. T. L. Ma, K. Inoue, K. Yao, H. Noma, T. Shuji, E. Abe, J. H. Yu, X. S. Wang and B. W. Zhang, *J. Electroanal. Chem.*, 2002, **537**, 31-38.
55. T. L. Ma, K. Inoue, H. Noma, K. Yao and E. Abe, J. Photochem. Photobiol. *A*, 2002, **152**, 207-212.
56. F. Odobel, E. Blart, M. Lagree, M. Villieras, H. Boujtita, N. El Murr, S. Caramori and C. A. Bignozzi, *J. Mater. Chem.*, 2003, **13**, 502-510.
57. J. A. Mikroyannidis, G. Charalambidis, A. G. Coutsolelos, P. Balraju and G. D. Sharma, *J. Power Sources*, 2011, **196**, 6622-6628.

58. M. K. Panda, G. D. Sharma, K. R. J. Thomas and A. G. Coutsolelos, *J. Mater. Chem.*, 2012, **22**, 8092-8102.
59. G. D. Sharma, M. K. Panda, M. S. Roy, J. A. Mikroyannidis, E. Gad and A. G. Coutsolelos, *Renew. Sust. Energ.*, 2013, **5**.
60. G. D. Sharma, P. A. Angaridis, S. Pipou, G. E. Zervaki, V. Nikolaou, R. Misra and A. G. Coutsolelos, *Org. Electron.*, 2015, **25**, 295-307.
61. C. Stangel, D. Daphnomili, T. Lazarides, M. Drev, U. O. Krasovec and A. G. Coutsolelos, *Polyhedron*, 2013, **52**, 1016-1023.
62. X. Wang, H. Wang, Y. Yang, Y. He, L. Zhang, Y. Li and X. Li, *Macromolecules*, 2010, **43**, 709-715.
63. C. Zhao, F. Ur Rehman, Y. Yang, X. Li, D. Zhang, H. Jiang, M. Selke, X. Wang and C. Liu, *Scientific Reports*, 2015, **5**, 11518.
64. A. Maruani, H. Savoie, F. Bryden, S. Caddick, R. Boyle and V. Chudasama, *Chem. Commun.*, 2015, **51**, 15304-15307.
65. A. J. Mozer, M. J. Griffith, G. Tsekouras, P. Wagner, G. G. Wallace, S. Mori, K. Sunahara, M. Miyashita, J. C. Earles, K. C. Gordon, L. Du, R. Katoh, A. Furube and D. L. Officer, *J. Am. Chem. Soc.*, 2009, **131**, 15621-15623.
66. J. K. Park, J. Chen, H. R. Lee, S. W. Park, H. Shinokubo, A. Osuka and D. Kim, *J. Phys. Chem. C*, 2009, **113**, 21956-21963.
67. G. E. Zervaki, M. S. Roy, M. K. Panda, P. A. Angaridis, E. Chrissos, G. D. Sharma and A. G. Coutsolelos, *Inorg. Chem.*, 2013, **52**, 9813-9825.
68. G. E. Zervaki, P. A. Angaridis, E. N. Koukaras, G. D. Sharma and A. G. Coutsolelos, *Inotg. Chem. Front.*, 2014, **1**, 256.
69. G. D. Sharma, G. E. Zervaki, K. Ladomenou, E. N. Koukaras, P. P. Angaridis and A. G. Coutsolelos, *J. Porphyrins Phthalocyanines*, 2015, **19**, 175-191.
70. G. D. Sharma, G. E. Zervaki, P. A. Angaridis, A. Vatikioti, K. S. V. Gupta, T. Gayathri, P. Nagarjuna, S. P. Singh, M. Chandrasekharam, A. Banthiya, K. Bhanuprakash, A. Petrou and A. G. Coutsolelos, *Org. Electron.*, 2014, **15**, 1324-1337.
71. V. Nikolaou, P. A. Angaridis, G. Charalambidis, G. D. Sharma and A. G. Coutsolelos, *Dalton Trans.*, 2015, **44**, 1734-1747.
72. G. E. Zervaki, E. Papastamatakis, P. A. Angaridis, V. Nikolaou, M. Singh, R. Kurchania, T. N. Kitsopoulos, G. D. Sharma and A. G. Coutsolelos, *Eur. J. Inorg. Chem.*, 2014, **2014**, 1020-1033.
73. G. E. Zervaki, A. Nikoforou, V. Nikolaou, G. D. Sharma and A. G. Coutsolelos, *J. Mater. Chem. C*, 2015, **3**, 5652-5664.
74. G. E. Zervaki, V. Tsaka, A. Vatikioti, I. Georgakaki, V. Nikolaou, G. D. Sharma and A. G. Coutsolelos, *Dalton Trans.*, 2015, **44**, 13550-13564.
75. C. Stangel, K. Ladomenou, G. Charalambidis, M. K. Panda, T. Lazarides and A. G. Coutsolelos, *Eur. J. Inorg. Chem.*, 2013, 1275-1286.
76. Y. Ooyama, S. Inoue, T. Nagano, K. Kushimoto, J. Ohshita, I. Imae, K. Komaguchi and Y. Harima, *Angew. Chem. Int. Edit.*, 2011, **50**, 7429-7433.
77. Y. Ooyama, T. Nagano, S. Inoue, I. Imae, K. Komaguchi, J. Ohshita and Y. Harima, *Chem. -Eur. J.*, 2011, **17**, 14837-14843.
78. J. F. Lu, X. B. Xu, Z. H. Li, K. Cao, J. Cui, Y. B. Zhang, Y. Shen, Y. Li, J. Zhu, S. Y. Dai, W. Chen, Y. B. Cheng and M. K. Wang, *Chem-Asian J*, 2013, **8**, 956-962.
79. D. Daphnomili, G. Landrou, S. P. Singh, A. Thomas, K. Yesudas, K. Bhanuprakash, G. D. Sharma and A. G. Coutsolelos, *RSC Adv.*, 2012, **2**, 12899-12908.
80. A. Yella, H. W. Lee, H. N. Tsao, C. Y. Yi and A. K. Chandiran, *Science*, 2011, **334**, 1203-1203.

81. W. M. Campbell, K. W. Jolley, P. Wagner, K. Wagner, P. J. Walsh, K. C. Gordon, L. Schmidt-Mende, M. K. Nazeeruddin, Q. Wang, M. Gratzel and D. L. Officer, *J. Phys. Chem. C*, 2007, **111**, 11760-11762.
82. G. D. Sharma, D. Daphnomili, K. S. V. Gupta, T. Gayathri, S. P. Singh, P. A. Angaridis, T. N. Kitsopoulos, D. Tasis and A. G. Coutsolelos, *RSC Adv.*, 2013, **3**, 22412-22420.
83. D. Daphnomili, G. D. Sharma, S. Biswas, K. R. J. Thomas and A. G. Coutsolelos, J. Photochem. Photobiol. *A*, 2013, **253**, 88-96.
84. S. Nakade, T. Kanzaki, W. Kubo, T. Kitamura, Y. Wada and S. Yanagida, *J. Phys. Chem. B*, 2005, **109**, 3480-3487.
85. G. Boschloo, L. Haggman and A. Hagfeldt, *J. Phys. Chem. B*, 2006, **110**, 13144-13150.
86. P. Wang, S. M. Zakeeruddin, R. Humphry-Baker and M. Gratzel, *Chem. Mater.*, 2004, **16**, 2694-2696.
87. G. D. Sharma, D. Daphnomili, P. A. Angaridis, S. Biswas and A. G. Coutsolelos, *Electrochim. Acta*, 2013, **102**, 459-465.
88. C. Stangel, A. Bagaki, P. A. Angaridis, G. Charalambidis, G. D. Sharma and A. G. Coutsolelos, *Inorg. Chem.*, 2014, **53**, 11871-11881.
89. C. J. Brabec, S. Gowrisanker, J. J. M. Halls, D. Laird, S. J. Jia and S. P. Williams, *Adv. Mater.*, 2010, **22**, 3839-3856.
90. M. Jorgensen, K. Norrman, S. A. Gevorgyan, T. Tromholt, B. Andreasen and F. C. Krebs, *Adv. Mater.*, 2012, **24**, 580-612.
91. Y. Li, *Acc. Chem. Res.*, 2012, **45**, 723-733.
92. T. Xu and L. Yu, *Mater. Today*, 2014, **17**, 11-15.
93. C. Cabanetos, A. El Labban, J. A. Bartelt, J. D. Douglas, W. R. Mateker, J. M. J. Frechet, M. D. McGehee and P. M. Beaujuge, *J. Am. Chem. Soc.*, 2013, **135**, 4656-4659.
94. K. H. Hendriks, G. H. L. Heintges, V. S. Gevaerts, M. M. Wienk and R. A. J. Janssen, *Angew. Chem. Int. Edit.*, 2013, **52**, 8341-8344.
95. L. Dou, C.-C. Chen, K. Yoshimura, K. Ohya, W.-H. Chang, J. Gao, Y. Liu, E. Richard and Y. Yang, *Macromolecules*, 2013, **46**, 3384-3390.
96. I. Osaka, T. Kakara, N. Takemura, T. Koganezawa and K. Takimiya, *J. Am. Chem. Soc.*, 2013, **135**, 8834-8837.
97. L. Ye, S. Zhang, W. Zhao, H. Yao and J. Hou, *Chem. Mater.*, 2014, **26**, 3603-3605.
98. Y. Liu, J. Zhao, Z. Li, C. Mu, W. Ma, H. Hu, K. Jiang, H. Lin, H. Ade and H. Yan, *Nat Commun*, 2014, **5**.
99. A. Mishra and P. Bäuerle, *Angew. Chem. Int. Ed.*, 2012, **51**, 2020-2067.
100. Y. Lin, Y. Li and X. Zhan, *Chem. Soc. Rev.*, 2012, **41**, 4245-4272.
101. Y. Chen, X. Wan and G. Long, *Acc. Chem. Res.*, 2013, **46**, 2645-2655.
102. J. Zhou, Y. Zuo, X. Wan, G. Long, Q. Zhang, W. Ni, Y. Liu, Z. Li, G. He, C. Li, B. Kan, M. Li and Y. Chen, *J. Am. Chem. Soc.*, 2013, **135**, 8484-8487.
103. V. S. Gevaerts, E. M. Herzig, M. Kirkus, K. H. Hendriks, M. M. Wienk, J. Perlich, P. Müller-Buschbaum and R. A. J. Janssen, *Chem. Mater.*, 2014, **26**, 916-926.
104. D. Liu, M. Xiao, Z. Du, Y. Yan, L. Han, V. A. L. Roy, M. Sun, W. Zhu, C. S. Lee and R. Yang, *J. Mater. Chem. C*, 2014, **2**, 7523-7530.
105. B. Kan, Q. Zhang, M. Li, X. Wan, W. Ni, G. Long, Y. Wang, X. Yang, H. Feng and Y. Chen, *J. Am. Chem. Soc.*, 2014, **136**, 15529-15532.
106. S.-W. Chiu, L.-Y. Lin, H.-W. Lin, Y.-H. Chen, Z.-Y. Huang, Y.-T. Lin, F. Lin, Y.-H. Liu and K.-T. Wong, *Chem. Commun.*, 2012, **48**, 1857-1859.

107. V. Steinmann, N. M. Kronenberg, M. R. Lenze, S. M. Graf, D. Hertel, K. Meerholz, H. Bürckstümmer, E. V. Tulyakova and F. Würthner, *Adv. Energy Mater.*, 2011, **1**, 888-893.
108. C. W. Tang and A. C. Albrecht, *Nature*, 1975, **254**, 507-509.
109. A. Goetzberger, C. Hebling and H.-W. Schock, *Materials Science and Engineering: Reports*, 2003, **40**, 1-46.
110. M. G. Walter, A. B. Rudine and C. C. Wamser, *J. Porphyrins Phthalocyanines*, 2010, **14**, 759-792.
111. M. V. Martinez-Diaz, G. de la Torre and T. Torres, *Chem. Commun.*, 2010, **46**, 7090-7108.
112. H. Imahori, T. Umeyama, K. Kurotobi and Y. Takano, *Chem. Commun.*, 2012, **48**, 4032-4045.
113. K. M. Kadish, K. M. Smith and R. Guilard, *Supramolecular Assemblies of Porphyrins and Phthalocyanines Derivatives for Solar Energy conversion and Molecular Electronics*, World Scientific Publishing Co. Pte. Ltd, 2014.
114. C.-L. Wang, W.-B. Zhang, R. M. Van Horn, Y. Tu, X. Gong, S. Z. D. Cheng, Y. Sun, M. Tong, J. Seo, B. B. Y. Hsu and A. J. Heeger, *Adv. Mater.*, 2011, **23**, 2951-2956.
115. Q. Sun, L. Dai, X. Zhou, L. Li and Q. Li, *Appl. Phys. Lett.*, 2007, **91**.
116. T. Oku, T. Noma, A. Suzuki, K. Kikuchi and S. Kikuchi, *J. Phys. Chem. Solids*, 2010, **71**, 551-555.
117. J. Hatano, N. Obata, S. Yamaguchi, T. Yasuda and Y. Matsuo, *J. Mater. Chem.*, 2012, **22**, 19258-19263.
118. Y. Y. Huang, L. S. Li, X. B. Peng, J. B. Peng and Y. Cao, *J. Mater. Chem.*, 2012, **22**, 21841-21844.
119. L. S. Li, Y. Y. Huang, J. B. Peng, Y. Cao and X. B. Peng, *J. Mater. Chem. A*, 2013, **1**, 2144-2150.
120. G. D. Sharma, D. Daphnomili, S. Biswas and A. G. Coutsolelos, *Org. Electron.*, 2013, **14**, 1811-1819.
121. G. D. Sharma, G. E. Zervaki, P. Angaridis and A. G. Coutsolelos, *RSC Adv.*, 2014, **4**, 50819-50827.
122. G. D. Sharma, S. A. Siddiqui, A. Nikiforou, G. E. Zervaki, I. Georgakaki, K. Ladomenou and A. G. Coutsolelos, *J. Mater. Chem. C*, 2015, **3**, 6209-6217.
123. G. D. Sharma, G. E. Zervaki, P. A. Angaridis, T. N. Kitsopoulos and A. G. Coutsolelos, *J. Phys. Chem. C*, 2014, **118**, 5968-5977.